Int J Clin Exp Med 2016;9(7):13394-13406
www.ijcem.com /ISSN:1940-5901/IJCEM0024478

Original Article

KLF15 is a positive regulatory factor in the process of myocardial remodeling and angiogenesis induced by pressure overload

Yang Yu[1], Shufan Zou[1], Qingjun Yang[2], Yingbin Xiao[1], Yu Yan[2], Hao Chen[2], Hongkun Wu[2], Yongjin Luo[2], Pengling Yu[2], Lin Chen[1]

[1]*Division of Cardiac Surgery, Xinqiao Hospital Affiliated to Third Military Medical University, Chongqing, PR China;* [2]*Zhongshan Hospital of Chongqing City, Chongqing, PR China*

Received January 19, 2016; Accepted May 4, 2016; Epub July 15, 2016; Published July 30, 2016

Abstract: Objectives: To elucidate the role of KLF15 on cardiac fibroblast in the dynamic angiogenesis in pressure-overload cardiac remodeling. Methods: Aortic banding was performed in rats to induce pressure-overload and cardiac hypertrophy. Part of the animals has their aorta constriction removed 3 or 6 weeks after the banding surgery. Cardiac function by echocardiography, cardiac tissue morphology and fibrosis, interstitial angiogenesis and KLF15 expression were measured. The effect of KLF15 on cardiac fibroblasts and vascular endothelial cells was determined *in vitro* using an over-expression system by KLF15 recombinant adenovirus to investigate the role of KLF15 in angiogenesis. Results: Pressure overload led to cardiac dysfunction, myocardial hypertrophy and fibrosis, accompanied with decreased capillary density. These phenotypes were associated with decreased cardiac expression level of KLF5. All cardiac dysfunction and hypertrophy phenotypes were slowed down or reversed by de-banding the constriction at an early stage (3 weeks after banding) together with a normalized cardiac KLF5 level, and partially reversed at a late stage (6 weeks after banding). *In vitro* over-expressing KLF15 in cardiac fibroblast promoted the formation of budding and tubular structure of endothelial cells in a three-dimensional co-cultures system, providing a potential causational relation between KLF15 and angiogenesis. Conclusion: Pressure-overload induced cardiac hypertrophy led to enhanced vascular angiogenesis which was possibly regulated by KLF15 base on both in vivo and in vitro data. Pressure-overload alleviation resulted in improved cardiac function, and partial reversal of fibrosis and angiogenesis with reversed KLF15 levels.

Keywords: Krüppel-like factor 15, pressure overload, myocardial remodeling, angiogenesis, three-dimensional culture

Introduction

Pressure and/or volume overload conditions like hypertension is highly related to the risk of developing chronic heart failure. Compensatory hypertrophy usually occurs at early stages of these patients and decompensated heart failure was a common event at the later stage [1]. There has been increasing evidence supporting the important role of angiogenesis in the pathogenesis of heart failure. Under normal circumstance, capillaries locate next to cardiomyocyte with vascular endothelial cells to cardiomyocytes of 3:1. Our published study showed that cardiac hypertrophy was associated with increased number of myocardial capillaries in the process of compensatory cardiac hypertrophy. In early 1941, Roberts et al. [2] reported that capillary density and degree of myocardial fibers were significantly lower in heart failure patients with cardiac hypertrophy. In a mouse model of Akt-induced myocardial hypertrophy, the degree of angiogenesis was directly related to cardiac size and function, suggesting that imbalance between hypertrophic myocardial tissue and angiogenesis could be a key event leading to heart failure. Evidence from our group and others also indicated the potential therapeutic value of blocking angiogenesis at an early stage through correcting the imbalance between capillaries numbers and myocardial fibers, an early transition stage related to later heart failure [3].

The Krüppel-like factors (KLFs) are a class of the most abundant and important transcriptional regulators in eukaryotes. Seventeen different members of KLF family have been reported, among which KLF15 is the most primary and important one [4] KLF15 is highly expressed in myocardium, vascular smooth muscle and skeletal muscle cells, and serves as an important factor in promoting the development of cardiovascular and sports systems. Several studies have shown that KLF15 inhibits myocardial hypertrophy and fibrosis, and also prevents cardiac ultrastructure change in myocardial remodeling including rearrangement of muscle fibers, interstitial fibrosis, extracellular matrix accumulation and angiogenesis [5]. However, among multiple pathogeneses through which KLF15 regulates cardiac hypertrophy, its role in regulating interstitial angiogenesis is considered to be the most important [6].

In the present study we used a pressure overload animal model to test the hypothesis that KLF15 is a positive regulatory factor in pressure overload-induced cardiac remodeling and angiogenesis. We further investigated the change of KLF15 levels and angiogenesis status after releasing the pressure overload through a second surgery to remove the aorta constriction. Also, we took the advantage of *in vivo* system to overexpress the KLF15 in cardiac fibroblast and studied its effect on angiogenesis.

Materials and methods

Animal model of pressure-induced overload and debanding

All procedures were strictly followed by the Guide of the use of Animals in Research, Testing and Education issued by the New York Academy of Sciences Ad Hoc Committee and 3R principle (Reduction, Refinement and Replacement). The Third Military Medical University experimental animal ethics committee approved all procedures.

Healthy male Sprague Dawley (SD) rats (Center of Laboratory Animal Medicine, the Third Military Medical University, PR China) were used for this study (body weight 100-150 g). After anesthetizing with 2% tribromoethanol (250 mg/kg, i.p.), [7] animals were secured on the operating table in the supine position and non-mechanically ventilated. Incisions into the skin and subcutaneous fascia covering the suprasternal fossae, on both sides, were made and the incision extended from external jugular vein medial edge down to the sternum at the level of second rib joint. Trachea was then exposed and sternum was lifted up with right angle forceps with thymus separated along the anterior wall of the trachea. This allowed the ascending aorta to be exposed and a suture was placed around the aorta using a calibration blunt needle, leading to a 50% reduction in the inner diameter of ascending aorta (aortic banding, AB). Aerosolized penicillin solution (10,000 units) was applied to the operation field and the chest was closed. At 3 weeks or 6 weeks after the first surgery which induced pressure-overload, second open-chest surgery was performed in part of the animals to remove the aortic band (aortic debading, AB+DB). In sham operation group, the ascending aorta was dissected but not ligated. All rats received daily treatment of penicillin (10,000 units) and buprenorphine (0.02 mg/kg) through intramuscular injection for 3 days after the operation. All rats were given a standard diet without restriction of drinking water.

Experimental rats were divided into the following six groups as follows: 1) Aortic banding 3w (AB3w) group which received pressure overload for 3 weeks; 2) Aortic banding 6w (AB6w) group which received pressure overload for 6 weeks; 3) Early aortic debanding (DB) group (AB3w+DB6w) which received a second surgery to remove the pressure overload for 6 weeks after a 3 weeks of pressure overload; 4) Advanced/late aortic debanding group (AB6w+DB6w) group, which received a second surgery to remove the pressure overload for 6 weeks after a 6 weeks of pressure overload; 5) Sham3w group which was sacrificed 3 weeks after the sham operation and 6) Sham6w which was sacrificed 6 weeks after sham operation.

Echocardiography for cardiac function and cardiac hypertrophy

All experimental rats were anaesthetized with tribromoethanol (50 mg/kg i.p.) [8]. Echocardiography was performed in all rats using 5500 Sonos, system (HP, USA) with a 15 MHz probe. Cardiac function parameters recorded included left ventricular end systolic diameter (LVESd), left ventricular end diastolic dimension (LVEDd),

inter ventricular septum at diastole (IVS) and left ventricular posterior wall thickness in diastole (LVPW). Left ventricular ejection fraction (EF) and left ventricular mass index (LVMI= [(ExLVDd^3-LVEDd^3)×1.055]/body mass) were calculated automatically by the software of 5500 Sonos system.

Histology staining

Left ventricle samples were fixed with 10% neutral formalin. After dehydration with graded ethanol solutions, specimens were collected, embedded in paraffin and sectioned (4 μm). All slices were stained by hematoxylin and eosin (HE). Histological changes in the myocardium were observed through a microscope. Sirius red staining was used to measure the degree of fibrosis in the cardiac tissue. The percentage of Sirius red (+) area in each section was quantified using Image J and 5 sections of each rat were used for quantification and statistical analysis.

Western blot

Total protein was extracted from culture cells with RIPA lysis buffer containing 50 mM Tris (pH 7.4), 150 mM NaCl, 1% TritonX-100, 1% sodium deoxycholate, 0.1% SDS, 2 mM sodium pyrophosphate, 25 mM β-glycerophosphate, 1 mM ethylene diamine tetraacetic acid (EDTA), 1 mM Na_3VO_4 and 0.5 μg/ml leupeptin. The concentration of protein samples was measured by Bicinchoninine acid assay (BCA). Samples were denatured with 5X SDS-polyacrylamide gel electrophoresis (SDS-PAGE) sample buffer. Protein samples were resolved by SDS-PAGE and transferred to polyvinylidene difluoride membrane. After blocking with 5% bovine serum albumin (BSA) at 37°C for 1 hour, membranes were incubated with primary antibody to KLF15 (1:200, from GeneTex) at 4°C for overnight. This was followed by being incubated with a secondary antibody (labeled with HRP) at 37°C for 1 hour. Finally, the protein bands were visualized using an immunohistochemical detection kit (from Abcam) and quantitatively analyzed using a gel image processing system (Bio-Rad, USA).

Real time quantitative PCR analysis (qPCR)

KLF15 and GAPDH mRNA levels were assessed by a q PCR. Total RNA from either cardiac tissue from rat or cultured cardiac fibroblast was extracted using RNAiso Plus kit (Takara, China). The cDNA synthesis reaction was performed with 1 μg of total RNA, PrimeScript RT Enzyme Mix I (Takara, China). Amplification and detection of specific gene was performed using SYBR® Premix Ex Taq II (Takara, China) with an iCycler Detection System (Bio-Rad, USA). The expression level of KLF15 gene was normalized to GAPDH as an internal control.

Immunofluorescence

After fixation in 4% paraformaldehyde and dehydration with a graded series of sucrose solutions, the left ventricle was embedded in paraffin and cut into sections. Histologic sections were incubated in 0.01 mol/L phosphate buffer solution (PBS, pH 7.4) for 10 min at room temperature, followed by incubations with a CD31 specific antibody (1:100, BD, USA) and secondary antibody (1:200, Sigma, USA) labeled with fluorescein isothiocyanate (FITC) at 37°C for 30 min. Sections were washed with PBS for 5 min, three times. After applying a drop of glycerol, the specific fluorescence intensity of each specimen was observed under the fluorescence microscopy (Leica, Germany) [9]. For each preparation, positive control (positive serum plus FITC), negative control (negative serum plus FITC) and fluorescent marker control (PBS plus FITC) were included for the purpose of quality control.

Cell culture

Left ventricular myocardium was obtained from neonatal SD rats (1-2 days of age) and cut into pieces. Minced tissue was digested with 0.25% trypsin in Hanks buffered saline solution (both from Gibco, USA) at 4°C overnight [10]. Cardiac fibroblasts were isolated and enriched by differential centrifugation (1500 *g*, 5 min) and then were plated in 20% DMEM/F12 medium (Gibco, USA) [11]. Cells were cultured in an incubator (Heraeus, Germany) set at 37°C and 5% carbon dioxide. According to the conditions of growth, the cardiac fibroblasts were passaged or frozen.

Primary rat aortic endothelia (RAE) were purchased from ATCC (USA) and endothelial cell growth medium-2 (EGM-2) was purchased from Lonza (Switzerland). The method of conventional vascular endothelial cell culture has been

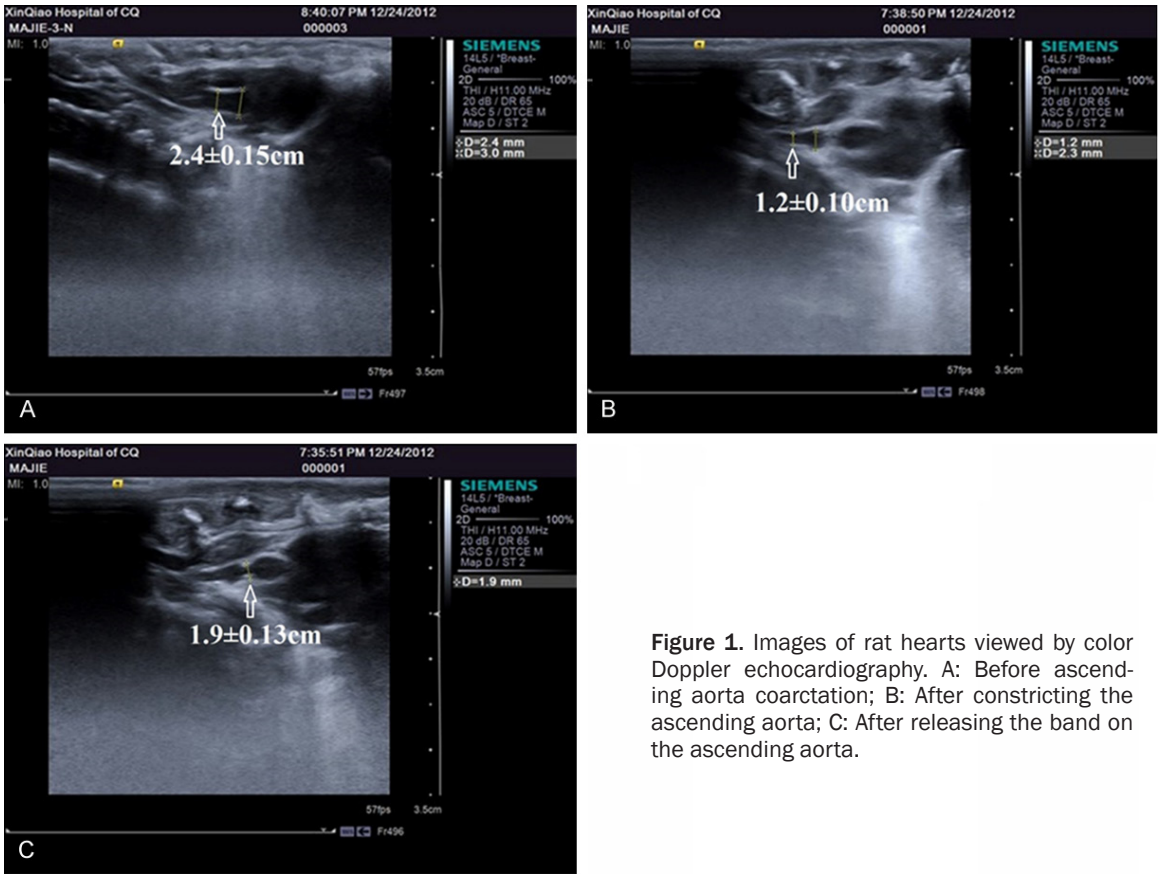

Figure 1. Images of rat hearts viewed by color Doppler echocardiography. A: Before ascending aorta coarctation; B: After constricting the ascending aorta; C: After releasing the band on the ascending aorta.

previously described [12] Cells from passages 3 to 5 were used in subsequent experiments.

Generation and use of KLF15 adenovirus

Rat KLF15 gene was amplified with specific primers (forward: 5'-CGTTGTGCTGCTTTCCTG-3' and reverse: 5'-GGAGGTGGGGGAGGGGAG-3'). The complete rat KLF15 cDNA was then cloned into the T vector pTA2 and transformed into DH10B *Escherichia coli*. Positive clones were verified by sequencing (Sangon). KLF15 was then sub-cloned into the adenovirus shuttle vector pAdTrack-CMV (cytomegalovirus) as previously described [13]. The pAdTrack-CMV-based plasmid harboring rat KLF-15 cDNA was co-transformed with an adeno-5 virus backbone (pAdEasy-1) into BJ5183 *E. coli*. Positive viral clones were purified by ultracentrifugation on CsCl-gradients, re-buffered in conservation buffer (TrisHCl 50 mM pH 8.3, glycerol 40%, $MgCl_2$ 5 mM, EDTA 0.1 mM pH 8), titrated, and stored at -80°C until further use. Titrations were performed using the limiting dilution method with viral suspensions and 911 cells [14].

Cardiac fibroblasts were infected with the pAdTrack-CMV adenovirus expressing KLF15 and its empty virus at a multiplicity of infection (MOF) of 100 for 2 days. Empty virus was used as control for KLF15 expression adenoviruses. The green fluorescent protein (GFP) was used as an infection success marker of both KLF15 and empty vectors. The efficiency of transfection was verified by western blot and qPCR.

Three-dimensional culture

Fibroblasts and vascular endothelial cells (ECs) were co-cultured in three-dimensional, 1% peptide hydrogel scaffolds (peptide sequence AcN-RARADADARARADADA-CNH2) [15]. Cells were seeded at a density of 1.4×10^6 cells/cm^2 in 1:1 ratio. In this case, cytokines or chemokines secreted by fibroblasts facilitated the ECs to migrate, sprout, and form three-dimensional capillary-like networks along the peptide hydrogel scaffold [16]. Specific methods used are explained as follows: RAE were digested with 0.25% trypsin containing EDTA and incubated in EGM at 37°C for 4 hours, fixed with 1% peptide hydrogel, and transferred to a 24-well cul-

Table 1. Echocardiographic assessment of experimental rats' heart function (n=10, $\bar{x}\pm s$)

		LVESd (mm)	LVEDd (mm)	IVS (mm)	LVPW (mm)	EF (%)	LVMI (mg/g)
AB3/6w	3w	2.93±0.42[a]	5.31±0.50[a]	2.35±0.32[a]	2.56±0.39[a]	47.93±3.82[a]	3.11±0.69[a]
	6w	3.25±0.61[a]	5.64±0.97[a]	2.75±0.48[a]	2.77±0.43[a]	41.02±4.17[a]	2.85±0.67[a]
AB3/6w+DB6w	3w	2.19±0.35[c]	4.37±0.49[c]	1.89±0.25[c]	2.12±0.38[c]	58.94±3.71[c]	2.27±0.82[c]
	6w	2.44±0.30[b,c,d]	4.80±0.52[b,c,d]	2.17±0.31[b,c,d]	2.34±0.24[b,c,d]	52.19±2.66[b,c,d]	2.46±0.42[b,c,d]
Sham	3w	2.05±0.27	4.20±0.50	1.61±0.29	1.92±0.26	63.44±5.46	2.09±0.84
	6w	2.07±0.34	4.25±0.53	1.63±0.28	2.01±0.27	64.62±3.37	1.06±0.44

NOTE: LVESd: Left ventricular end systolic diameter; LVEDd: Left ventricular end diastolic dimension; IVS: Inter ventricular septum at diastole; LVPW: Left ventricular posterior wall thickness in diastole; EF: Left ventricular ejection fractions; LVMI: Left ventricular mass index. [a]P<0.01 when compared with sham groups; [b]P<0.01 when compared with sham groups; [c]P<0.05 when compared with time-point matched AB groups; [d]P<0.05 when compared with AB3w+DB6w.

Table 2. The ratio of left ventricular weight to body weight in experimental rats (n=10, $\bar{x}\pm s$)

		LVW (mg)	BW (g)	LVW/BW (mg/g)
AB3/6w	3w	802.75±190.22[a]	286.08±14.65	2.80±0.59[a]
	6w	1272.22±110.72[a]	421.34±12.34[a]	3.02±0.24[a]
AB3/6w+DB6w	3w	1247.97±146.45[b,c]	581.03±14.90[b,c]	2.15±0.28[b,c]
	6w	1840.63±261.57[b,c,d]	734.12±16.34[b,c,d]	2.51±0.33[b,c,d]
Sham3/6w	3w	379.01±131.29	290.03±15.62	1.32±0.49
	6w	460.86±170.13	415.44±14.32	1.10±0.39

Note: LVW: Left ventricular weight; BW: Body weight. [a]P<0.01 when compared with sham groups; [b]P<0.01 when compared with sham groups; [c]P<0.05 when compared with time-point matched AB groups; [d]P<0.05 when compared with AB3w+DB6w.

ture plate. After a 30 minutes treatment of thrombin, cardiac fibroblasts with or without KLF15 overexpression were added to the coagulated gels and co-cultured with ECs for up to 7 days at 37°C and 5% CO_2 in culture medium (10% fetal calf serum). The medium was changed on days 2, 4, and 6. After removing the medium, samples from the two groups were fixed with 4% paraformaldehyde and prepared for further study.

Fluorescent immunohistochemistry

Cells from the above three-dimensional vessel model system were washed with PBS (0.01 mol/L, pH 7.4) three times to remove paraformaldehyde, followed by being staining with FITC-lectin (10 ug/ml, Sigma, USA) at room temperature for 30 min. Fluorescence microscopy (Leica, Germany) was used to observe the three-dimensional cells preparations and images were taken [17].

Statistical analyses

The experimental data were represented as the mean ± standard deviation. All data were analyzed using SAS8.0v statistical software. Experiments with multiple groups were analyzed with a one-way ANOVA, followed by post-hoc analysis to analyze the difference between two specific groups. Experiments comparing two groups were analyzed using t test. Two tail $P<0.05$ was considered as statistically significant.

Results

General situation of rat model

Although aortic banding model is a broadly used pressure overload model to investigate cardiac remodeling, removal of pressure overload by debanding the constriction has not been commonly used to investigate the effect of reversal of pressure overload on cardiac remodeling. Our study showed that animal could survive two consequent surgeries successfully. Two and three animals from AB3w group and AB6w groups, respectively, died within one week after the surgery. Two animals in the AB6w+DB6w group died after the second surgery of debanding. Altogether, the banding and debanding groups shared similar mortality.

Echocardiograph and left ventricular weight/body weight ratio before and after debanding to remove the pressure overload

The color Doppler echocardiography showed that the diameter of the ascending aorta was approximately 2.4±0.15 cm in Sham group animals without ascending aorta banding and ves-

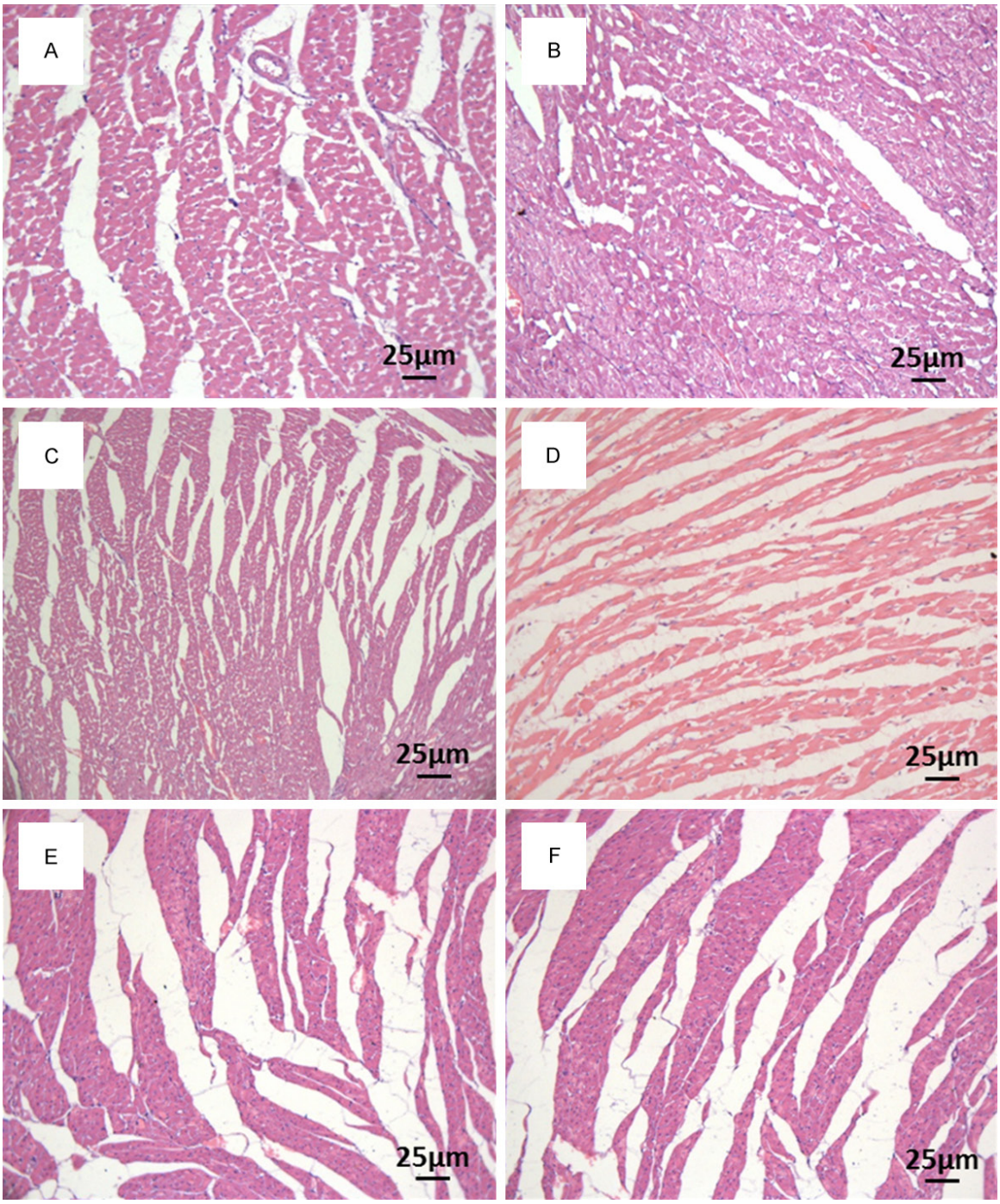

Figure 2. HE staining of the left ventricular myocardium following pressure overload or unload. A: AB3w, pressure overload for 3 weeks; B: AB6w, pressure overload for 6 weeks; C: AB3w+DB6w, unload for 6 weeks after pressure overload for 3 weeks; D: AB6w+DB6w, unload for 6 weeks after pressure overload for 6 weeks; E: Sham3w, sham operation for 3 weeks; F: Sham6w, sham operation for 6 weeks.

sel wall showed smooth ultrasound signaling without thickness (**Figure 1A**). After ascending aorta constriction, the vessel lumen was stenotic with diameter decreasing to half of the normal value, approximately 1.2±0.10 cm ($P<0.001$ vs. Sham groups (**Figure 1B**). After debanding the aorta constriction, the ascending aortic diameter increased significantly compared with banding group, reaching approximately 1.9±0.13 cm in diameter ($P<0.001$ vs.

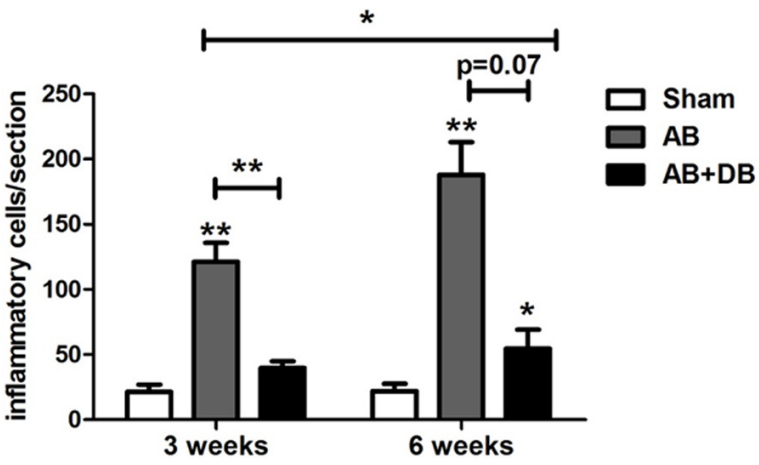

Figure 3. Quantification inflammatory cell infiltration into cardiac tissue of rats in each group.

AB groups) (**Figure 1C**) and indicating a successful debanding.

In the AB group, the myocardium presented concentric hypertrophy, and the heart function notably declined. AB caused a significant increase in LVESd, LVEDd, IVS, LVPW, LVMI and LVW/BW, and decreased EF compared to the sham group (all P<0.01) (**Table 1**), suggesting cardiac dysfunction. Cardiac hypertrophy reflected by IVS, LVPW and LVMI were significantly improved in the AB+DB groups when compared with AB groups at the matched time points (all P<0.05 vs. AB group) (**Table 1**). Besides, debanding, which release the pressure overload, also led to a better cardiac function reflected by a significantly decreased LVESd and LVEDd, and a significantly increased EF (all P<0.05 vs. AB groups) (**Table 1**). Moreover, earlier correction of pressure overload led to a better cardiac function (P<0.05 between AB3w+DB6w vs. AB6w+DB6w for all parameters in **Table 1**).

More importantly, cardiac hypertrophy (IVS, LVPW and LVMI values) was significantly decreased in AB3w+DB6w group and systolic heart function (EF) was significantly improved compared with those of AB6w+DB6w group, indicating that the earlier the pressure overload was removed, the better the heart function would be (**Table 1**, AB3wk+DB6w and AB6w+DB6w groups). Similarly, cardiac hypertrophy parameters including LVW and LVW/BW gradually but significantly increased after pressure overload for 6 weeks (**Table 2**). However, removal of pressure overload by debanding at 3 week time point led to a significantly decreased LVW/BW and LVW compared with those debanding performed at 6 week time point (**Table 2**).

Morphology and fibrosis change of cardiac tissues

Compared with sham groups, HE staining of the left ventricular myocardium from the AB group rats showed cardiomyocyte hypertrophy, inflammatory cell infiltration, disorder arrangement of myocardial fibers and interstitial hyperplasia (**Figure 2A**, **2B**, **2E** and **2F**). Unloading the ascending aorta reversed the hypertrophy to a normal level (**Figure 2C**, **2D**).

Since inflammatory cell infiltration had been reported in rat pressure overload model and cardiac inflammation was an important profibrogenic stimulus for cardiac hypertrophy and dysfunction, we further checked the inflammatory cell infiltration in our banding and debanding models. We found that pressure overload led to an enhanced inflammatory cells infiltration into cardiac tissue in a time dependent manner. Removal of aortic constriction at an early stage (3 week time point) significantly decreased the inflammatory cells infiltration (P<0.01), while at a relatively late stage (6 week time point), debanding was associated with a board line decreased inflammatory cells infiltration when compared with AB group (P=0.07 between AB 6w group and AB+DB6w group) (**Figure 3**).

Similar to the finding of HE staining, the fibrosis of rats challenged with pressure-overload for 3 weeks developed interstitial fibrosis (P<0.05 vs. Sham 3 weeks) and prolonged pressure-overload for 6 weeks led to a further deterioration of cardiac fibrosis (P<0.05 vs. Sham 3 weeks and Sham 6 weeks) (**Figure 4B**, **4E-G**). In contrast, removal of pressure-overload at an earlier or later stage resulted in a much less degree of cardia fibrosis (P<0.05 vs. AB3w+DB6w and AB6w+DB6w; **Figure 4C**, **4E-G**), suggesting a beneficial role of reducing pressure overloading in protecting cardiac fibrosis.

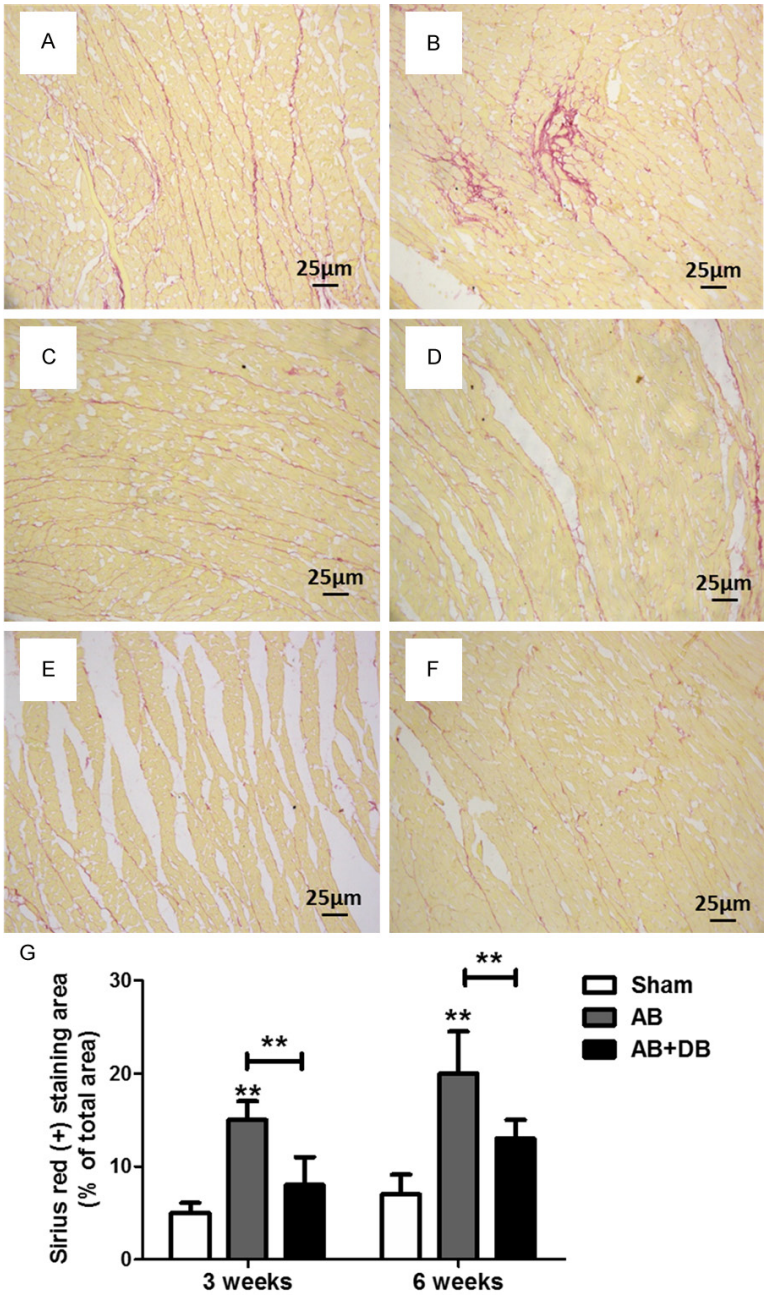

Figure 4. Cardiac fibrosis of animals in each group. A: AB3w, pressure overload for 3 weeks; B: AB6w, pressure overload for 6 weeks; C: AB3w+DB6w, unload for 6 weeks after pressure overload for 3 weeks; D: AB6w+DB6w, unload for 6 weeks after pressure overload for 6 weeks; E: Sham3w, sham operation for 3 weeks; F: Sham6w, sham operation for 6 weeks; G: Quantification with statistical analysis.

KLF15 gene expression levels in cardiac tissues of rats

Both AB and AB+DB groups had significantly decreased KLF15 mRNA levels compared with those of their time point matched Sham group ($P<0.01$) (**Figure 5**, $^{**}P<0.01$ between indicated groups). However, mRNA levels of KLF15 in AB3w+DB6w group significantly increased when compared with either AB groups or AB6w+DB6w ($P<0.01$), but not significantly change compared with Sham groups, suggesting that debanding to reduce the pressure overload was associated with normalized KLF15 mRNA levels. In addition, removal of pressure overload at a later time point (6 weeks after pressure overload) was able to partially reverse the decreased KLF15 levels, without reaching the statistical significance, indicating that controlling pressure overload at early stage of disease development is of vital importance.

Angiogenesis in cardiac tissues of rats with and without AB or AB+DB

The microvascular density (MVD) significantly decreased in AB group reflected by CD31+ micro-vessel (**Figure 6A-D**) compared with that of Sham group (**Figure 6E**, **6F**). However, the MVD of AB+DB rat hearts increased compared to time point matched AB rats (AB3w vs. AB3W+DB6w and AB6w vs. AB6w+DB6w, **Figure 6A-D** and **6G**), suggesting a reversal of MVD after pressure overload removal. More importantly, the MVD level of rats in AB3w+DB6w group was completely normalized to that of the 3 weeks Sham group, which was not the case for AB6w+DB6w group. These data was consistent with the KLF15 mRNA levels, suggesting again that early intervention of pressure overload correction is of vital important.

Verified KLF15 adenovirus and empty virus transfection

Cardiac fibroblasts transfected with KLF15 or empty adenovirus attached with GFP tag show-

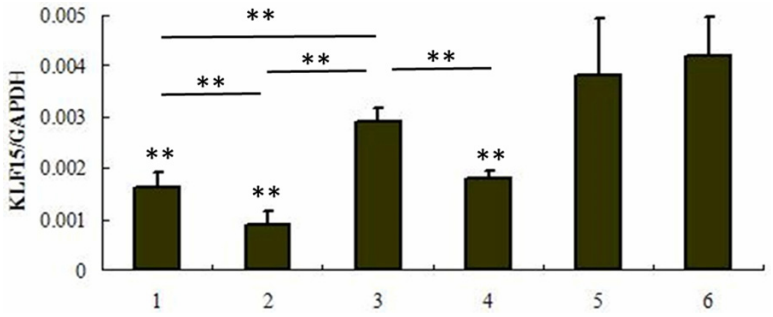

Figure 5. Levels of KLF15 mRNA in rat hearts following pressure overload. 1. AB3w, pressure overload for 3 weeks; 2. AB6w, pressure overload for 6 weeks; 3. AB3w+DB6w, unload for 6 weeks after pressure overload for 3 weeks; 4. AB6w+DB6w, unload for 6 weeks after pressure overload for 6 weeks; 5. Sham3w, sham operation for 3 weeks; 6. Sham6w, sham operation for 6 weeks. **P<0.01 between indicated two groups, or P<0.01 vs. time point matched Sham group.

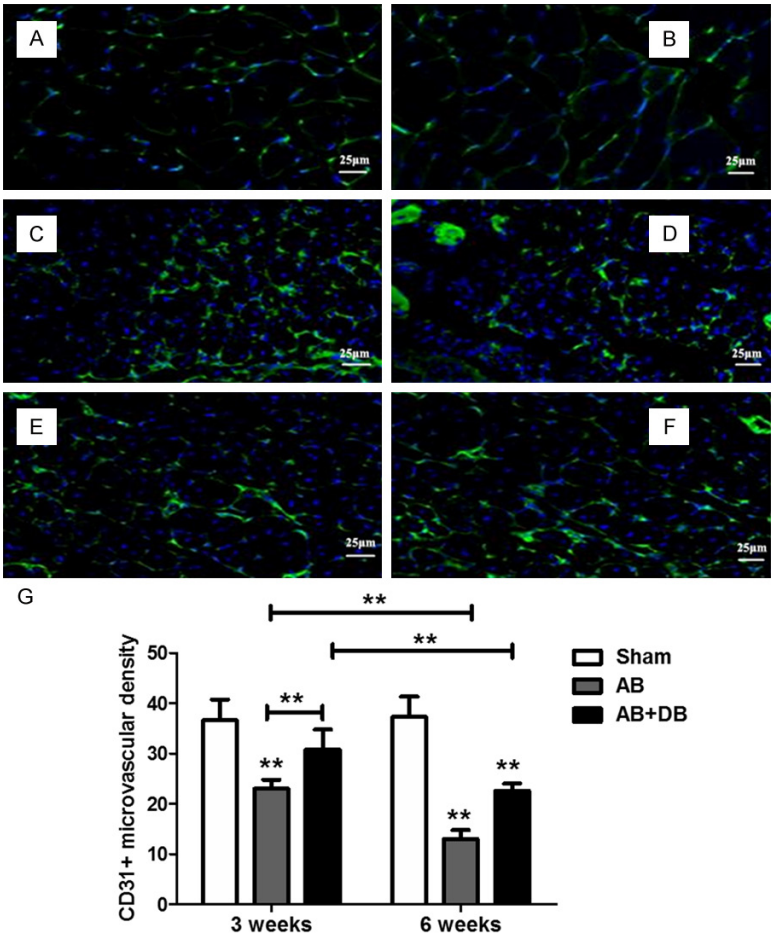

Figure 6. CD31 in left ventricular myocardium of experimental rats detected by Immunofluorescence. A: AB3w, pressure overload for 3 weeks; B: AB6w, pressure overload for 6 weeks; C: AB3w+DB6w, unload for 6 weeks after pressure overload for 3 weeks; D: AB6w+DB6w, unload for 6 weeks after pressure overload for 6 weeks; E: Sham3w, sham operation for 3 weeks; F: Sham6w, sham operation for 6 weeks; G: Quantification and statistical analysis. **P<0.01 vs. time point matched Sham group or between two indicated groups.

ed positive stain of GFP, indicating a success adenovirus transfection (**Figure 7A**, **7B**). To further validate the transfection efficiency of KLF15 adenovirus and empty virus, we performed western blot and qPCR to check KLF15 protein and gene expression levels. We found that KLF15 protein and mRNA in KLF15 vector group was much higher than those of the empty virus group (P<0.01) (**Figure 7C**, **7D**), confirming the success transfection.

Positive regulation of vascular endothelial cells by KLF15

Co-culturing endothelial cells with cardiac fibroblasts transfected with KLF15 vector or empty vector showed that endothelial cells co-cultured with KLF15 overexpressing cardiac fibroblast had a better morphology of tubular structures formation (**Figure 8A**, **8B**) when compared with cells transfected with empty vectors (**Figure 8C**, **8D**). Further quantification showed that the length of tubular structure in KLF15 vector group was 855±67 μm, significantly longer than that of the empty vector group (521±36 μm, P<0.01) (data not shown).

Discussion

Cardiovascular disease (CVD), particularly heart failure, is the leading cause of death globally. Among various causes of heart failure, pressure and/or volume overload-induced cardiac hypertrophy is the most common pathological change due to the high incidence of hypertension and ischemic heart disease. When cardiac hypertrophy takes place, cardiac myocytes increase in size and enhance in protein

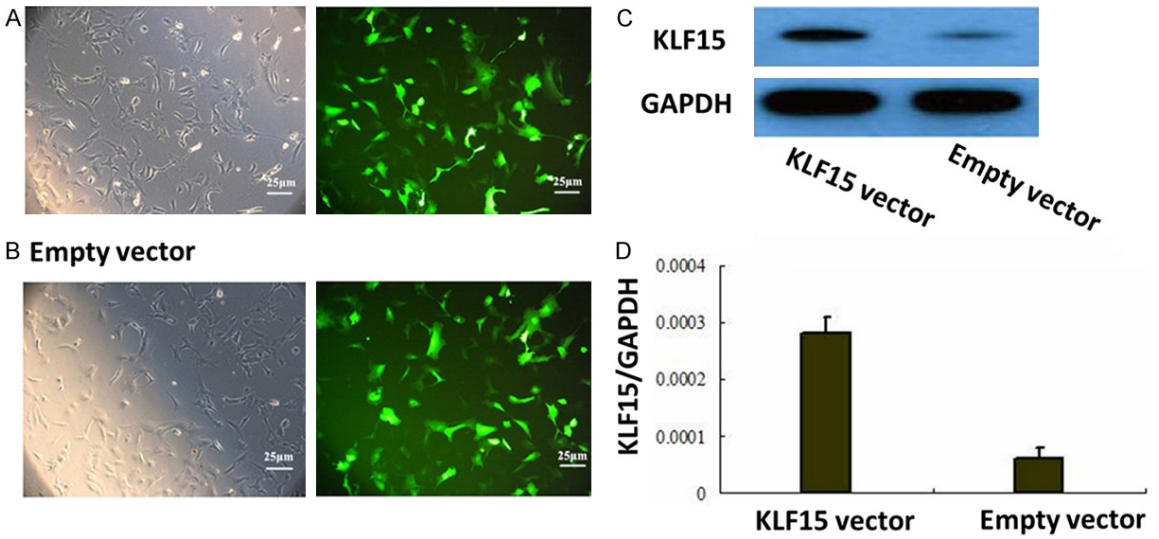

Figure 7. KLF15 transfection of cardiac fibroblast. A, B: GFP positive cardiac fibroblast after trasfect with KLF15 vector A: and empty vector B: both of which has GPF. C: protein level of KLF15 protein in two groups of cardiac fibroblasts as assessed by western blot analysis. D: mRNA level of KLF15 in two groups of cardiac fibroblasts as assessed by qPCR.

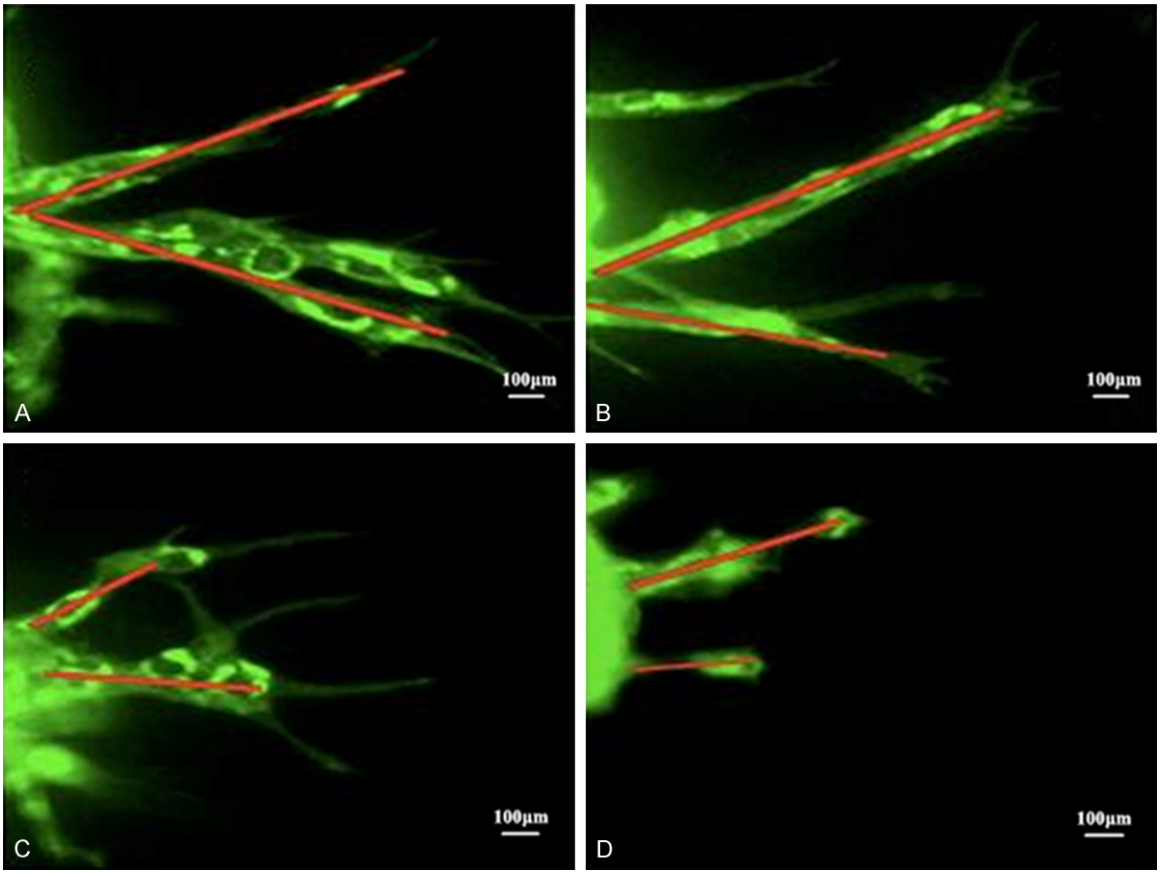

Figure 8. KLF15 promotes vessel formation in vascular endothelial cells cultured in three-dimensions. Two groups of cells grown in three-dimensional vessel models were stained with specific lectin. A, B: KLF15-CFs-RAE- Peptide Hydrogel group; C, D: Empty virus-CFs-RAE- Peptide Hydrogel group.

synthesis, while several other pathological change in interstitial tissues and cardiac fibroblasts also take place including fibrosis and angiogenesis. Studies have demonstrated cardiac myocyte as a source of vascular endothelial growth factor (VEGF), an important growth factor in regulating endothelial cell growth and angiogenesis. This suggests that cardiomyocytes under pressure overload could regulate angiogenesis through certain signaling pathways [18]. In a mouse model of Akt-induced myocardial hypertrophy, researchers showed that hypertrophic stimuli induced the expression of angiogenic growth factors such as VEGF in the adaptive phase of the hypertrophic remodeling, and blockade of VEGF signaling resulted in a reduction in capillary density and an early development of heart failure [19]. Another study demonstrated that VEGF deficiency led to a reduction in myocardial capillary density and accelerated compensatory cardiac hypertrophy [20]. These studies indicated that under physiological or compensatory hypertrophy conditions, growth-promoting signals could be important in stimulating hypertrophy and angiogenic growth factor expression in myocytes, which also served as a vital mechanism in maintaining the balance between myocyte hypertrophy and coronary angiogenesis. Once the balance is disrupted and myocardial angiogenesis is impaired, decompensated heart failure would happen [21].

Angiogenesis is related to the secretion of a variety of angiogenic factors by myocardial cells by pressure overload (mechanically) and/or hypoxia (chemically), from [22]. These cytokines caused vascular basement membrane degradation, endothelial cell activation, proliferation, migration, and the ultimate formation of new vascular networks [3]. New blood vessels provided the necessary supply of oxygen and nutrients to the remodeling myocardium. Under normal physiological conditions, the balance between angiogenesis inducers and inhibitors maintained. Under pathophysiological conditions, for example hypertrophy or myocardial interstitial fibrosis and, this balance disturbed such that angiogenesis was blocked, and consequently heart function deteriorated [23].

Many kinds of cells, growth factors and enzymes are involved in the complex control systems that regulate angiogenesis. Cardiac tissue is mainly composed of three types of cells: cardiomyocytes, cardiac fibroblasts and endothelial cells. Cardiac fibroblasts play a crucial role in the setting of pathological cardiac hypertrophy. In addition to the enlargement of individual cardiomyocytes and rearrangement of muscle fibers, interstitial fibrosis and angiogenesis occur and are part of the complex structural remodeling that occurs in the hypertrophic myocardium [24]. These studies highlight an important role of non-muscle cells, which reside in the intersititium, in the remodeling process associated with cardiac hypertrophy. A large number of studies have demonstrated that cardiac fibroblasts and cardiac myocytes, through the interaction of many cytokines, regulate angiogenesis during the myocardial remodeling process. At the same time, direct cell-cell contact between cardiomyocytes, cardiac fibroblasts and endothelial cells is also an important mechanism for promoting angiogenesis [25].

KLF15 is a member of the KLF family of transcription factors. Seventeen KLF basic regulation factors have been identified. The study of Leenders et al. confirmed that transforming growth factor-β (TGF-β) could inhibit the expression of KLF15 through the activation of p38 mitogen activated protein kinase (p38-MAPK) in cardiomyocytes [26]. This study also demonstrated that KLF15 could combine with myocardin, competitively, reduce the content of free serotonin, and, thereby, inhibit transcriptional regulation by serum response factor (SRF) and downstream cardiomyocyte hypertrophy [26]. Myocardin-related transcription factor A (MRTF-A/MKL1), as the key factor of SRF, is an important regulator of interstitial fibrosis in cardiac fibroblasts [27]. Through the bioinformatics analysis of the identified KLF15 region that combines with myocardin it was found that MRTF-A has a similar protein domain as the region in KLF15 that binds to myocardin. Therefore, KLF15 may be a competitive binding factor for MRTF-A in cardiac fibroblasts and act as in inhibitory factor for the development of interstitial fibrosis [28]. However, from the research using the cardiac hypertrophy model, KLF15 can also significantly inhibit the expression of connective tissue growth factor (CTGF) by cardiac fibroblasts. This KLF15 mechanism of action is presumably related to transactivation of the CTGF promoter through the competi-

tive inhibition of smad3 phosphorylation by KLF15. This mechanism could also likely be important for inhibiting myocardial hypertrophy [29]. Thus, KLF15 plays a key role in the process of inhibiting myocardial hypertrophy and fibrosis. The question remains as to how it potentially regulates angiogenesis.

We have observed the heart dysfunction and myocardial fibrosis in pressure overload model which was associated with decreased interstitial angiogenesis and KLF15 expression level, suggesting a possible role of KLF15 in cardiac hypertrophy through regulating angiogenesis. Correction of pressure overload at an earlier stage of cardiac hypertrophy by debanding the aorta constriction led to slow down of cardiac dysfunction and less severe myocardial fibrosis, accompanied with reversed cardiac KLF15 level and angiogenesis, indicating a further role of KLF15 in regulating angiogenesis. Our in vitro experiment using transfection of cardiac fibroblasts with KLF15 adenovirus successfully recapitulate the association between up-regulated the expression of KLF15 and angiogenesis in vitro, providing evidence of a possible causational relationship between KLF15 and angiogenesis.

Conclusion

We found in this study that under the stimulation of cardiac pressure overload, expression of KLF15 in cardiac tissue was reduced, which was associated with reduced cardiac angiogenesis. Unloading pressure at an early stage of the disease progression rather than a later stage could largely reverse the pathological change of the heart tissue and cardiac function, with reversed cardiac KLF15 level and angiogenesis. Therefore, we speculate that KLF15-related angiogenesis can be used as an effective target of gene therapy for patients with advanced heart failure at an early stage. However, the understanding of the underlining mechanism needs further investigation before any defined conclusion could be drawn.

Disclosure of conflict of interest

None.

Address correspondence to: Dr. Lin Chen, Division of Cardiac Surgery, Xinqiao Hospital Affiliated to Third Military Medical University, Chongqing, PR China. Tel: +86-23-68774107; Fax: 023-68774107; E-mail: chenlin_xinwaike@hotmail.com (primary); chenlin_xinwaike@yahoo.com

References

[1] Laroumanie F, Douin-Echinard V, Pozzo J, Lairez O, Tortosa F, Vinel C, Delage C, Calise D, Dutaur M, Parini A, Pizzinat N. CD4+ T Cells Promote the Transition from Hypertrophy to Heart Failure During Chronic Pressure Overload. Circulation 2014; 129: 2111-2124.

[2] Roberts JT, Wearn JT. Quantitative changes in the capillary-muscle relationship in human hearts during normal growth and hypertrophy. Am Heart J 1941; 21: 617-633.

[3] Oka T, Akazawa H, Naito AT, Komuro I. Angiogenesis and cardiac hypertrophy: maintenance of cardiac function and causative roles in heart failure. Circ Res 2014; 114: 565-571.

[4] Haldar SM, Ibrahim OA, Jain MK. Kruppel-like Factors (KLFs) in muscle biology. J Mol Cell Cardiol 2007; 43: 1-10.

[5] Fisch S, Gray S, Heymans S, Haldar SM, Wang B, Pfister O, Cui L, Kumar A, Lin Z, Sen-Banerjee S, Das H, Petersen CA, Mende U, Burleigh BA, Zhu Y, Pinto YM, Liao R, Jain MK. Kruppel-like factor 15 is a regulator of cardiomyocyte hypertrophy. Proc Natl Acad Sci U S A 2007; 104: 7074-7079.

[6] Haldar SM, Lu Y, Jeyaraj D, Kawanami D, Cui Y, Eapen SJ, Hao C, Li Y, Doughman YQ, Watanabe M, Shimizu K, Kuivaniemi H, Sadoshima J, Margulies KB, Cappola TP, Jain MK. Klf15 deficiency is a molecular link between heart failure and aortic aneurysm formation. Sci Transl Med 2010; 2: 26ra26.

[7] Kathleen J, Maherasa, Alexander G. Increased anesthesia time using 2, 2, 2-tribromoethanol-chloral hydrate with low impact on mouse psychoacoustics. J Neurosci Methods 2013; 219: 61-69.

[8] Feldman AM, Francis GS, Ganiats TG, Jessup M, Konstam MA, Mancini DM, Michl K, Oates JA, Rahko PS, Silver MA, Stevenson LW, Yancy CW; American College of Cardiology Foundation; American Heart Association. 2009 focused update incorporated into the ACC/AHA 2005 Guidelines for the Diagnosis and Management of Heart Failure in Adults: a report of the American College of Cardiology Foundation /American Heart Association Task Force on Practice Guidelines: developed in collaboration with the International Society for Heart and Lung Transplantation. Circulation 2009; 119: e391-479.

[9] Karamanolis G, Delladetsima I, Kouloulias V, Papaxoinis K, Panayiotides I, Haldeopoulos D, Triantafyllou K, Kelekis N, Ladas SD. Increased

expression of VEGF and CD31 in postradiation rectal tissue: implications for radiation proctitis. Mediators Inflamm 2013; 2013: 515048.
[10] Laskowski A, Woodman OL, Cao AH, Drummond GR, Marshall T, Kaye DM, Ritchie RH. Antioxidant actions contribute to the antihypertrophic effects of atrial natriuretic peptide in neonatal rat cardiomyocytes. Cardiovasc Res 2006; 72: 112-123.
[11] Xu H, Yi BA, Wu H, Bock C, Gu H, Lui KO, Park JH, Shao Y, Riley AK, Domian IJ, Hu E, Willette R, Lepore J, Meissner A, Wang Z, Chien KR. Highly efficient derivation of ventricular cardiomyocytes from induced pluripotent stem cells with a distinct epigenetic signature. Cell Res 2012; 22: 142-154.
[12] Herwig MC, Tsokos M, Hermanns MI, Kirkpatrick CJ, Müller AM. Vascular endothelial cadherin expression in lung specimens of patients with sepsis-induced acute respiratory distress syndrome and endothelial cell cultures. Pathobiology 2013; 80: 245-251.
[13] He TC, Zhou S, da Costa LT, Yu J, Kinzler KW, Vogelstein B. A simplified system for generating recombinant adenoviruses. Proc Natl Acad Sci U S A 1998; 95: 2509-2514.
[14] Grigorov B, Rabilloud J, Lawrence P, Gerlier D. Rapid titration of measles and other viruses: optimization with determination of replication cycle length. PLoS One 2011; 6: e24135.
[15] Cho H, Balaji S, Sheikh AQ, Hurley JR, Tian YF, Collier JH, Crombleholme TM, Narmoneva DA. Regulation of endothelial cell activation and angiogenesis by injectable peptide nanofibers. Acta Biomater 2012; 8: 154-164.
[16] Correia C, Grayson WL, Park M, Hutton D, Zhou B, Guo XE, Niklason L, Sousa RA, Reis RL, Vunjak-Novakovic G. In vitro model of vascularized bone: synergizing vascular development and osteogenesis. PLoS One 2011; 6: e28352.
[17] Jiang Y, Wang H, Culp D, Yang Z, Fotheringham L, Flannery J, Hammond S, Kafri T, Hartnett ME. Targeting Müller cell-derived VEGF164 to reduce intravitreal neovascularization in the rat model of retinopathy of prematurity. Invest Ophthalmol Vis Sci 2014; 55: 824-831.
[18] Kwasiborski PJ, Kowalczyk P, Mrówka P, Kwasiborski M, Cwetsch A, Przybylski J. Selected, biochemical markers of hypoxia. Przegl Lek 2012; 69: 115-119.
[19] Wang B, Yang Q, Bai WW, Xing YF, Lu XT, Sun YY, Zhao YX. Tongxinluo protects against pressure overload-induced heart failure in mice involving VEGF/Akt/eNOS pathway activation. PLoS One 2014; 9: e98047.
[20] Rengo G, Cannavo A, Liccardo D, Zincarelli C, de Lucia C, Pagano G, Komici K, Parisi V, Scala O, Agresta A, Rapacciuolo A, Perrone Filardi P, Ferrara N, Koch WJ, Trimarco B, Femminella GD, Leosco D. Vascular endothelial growth factor blockade prevents the beneficial effects of β-blocker therapy on cardiac function, angiogenesis, and remodeling in heart failure. Circ Heart Fail 2013; 6: 1259-1267.
[21] Shiojima I, Sato K, Izumiya Y, Schiekofer S, Ito M, Liao R, Colucci WS, Walsh K. Disruption of coordinated cardiac hypertrophy and angiogenesis contributes to the transition to heart failure. J Clin Invest 2005; 115: 2108-2118.
[22] Choi YH, Cowan DB, Nathan M, Poutias D, Stamm C, del Nido PJ, McGowan FX Jr. Myocardial hypertrophy overrides the angiogenic response to hypoxia. PLoS One 2008; 3: e4042.
[23] Kuang L, Feng J, He G, Jing T. Knockdown of Nrf2 inhibits the angiogenesis of rat cardiac micro-vascular endothelial cells under hypoxic conditions. Int J Biol Sci 2013; 9: 656-665.
[24] McConnell BB, Yang VW. Mammalian Kruppel-like factors in health and diseases. Physiological Reviews 2010; 90: 1337-1381.
[25] Howard CM, Baudino TA. Dynamic cell-cell and cell-ECM interactions in the heart. J Mol Cell Cardiol 2014; 70: 19-26.
[26] Xu R, Lin F, Zhang S, Chen X, Hu S, Zheng Z. Signal pathways involved in reverse remodeling of the hypertrophic rat heart after pressure unloading. Int J Cardiol 2010; 143: 414-423.
[27] Leenders JJ, Wijnen WJ, Hiller M, van der Made I, Lentink V, van Leeuwen RE, Herias V, Pokharel S, Heymans S, de Windt LJ, Høydal MA, Pinto YM, Creemers EE. Regulation of cardiac gene expression by KLF15, a repressor of myocardin activity. J Biol Chem 2010; 285: 27449-27456.
[28] Small EM, Thatcher JE, Sutherland LB, Kinoshita H, Gerard RD, Richardson JA, Dimaio JM, Sadek H, Kuwahara K, Olson EN. Myocardin-related transcription factor-a controls myofibroblast activation and fibrosis in response to myocardial infarction. Circ Res 2010; 107: 294-304.
[29] Wang B, Haldar SM, Lu Y, Ibrahim OA, Fisch S, Gray S, Leask A, Jain MK. The Kruppel-like factor KLF15 inhibits connective tissue growth factor (CTGF) expression in cardiac fibroblasts. J Mol Cell Cardiol 2008; 45: 193-197.